




Highly efficient, recyclable cerium-phosphate solid acid catalysts for the synthesis of tetrahydrocarbazole derivatives by Borsche–Drechsel cyclization

Hatem M. Altass^{1,2} · Abdelrahman S. Khder^{1,2,3}  · Saleh A. Ahmed^{1,2,4} · Moataz Morad^{1,2} · Abdullah A. Alsabei^{1,2} · Rabab S. Jassas⁵ · Khalid Althagafy^{2,6} · Awad I. Ahmed³ · Reda S. Salama⁷

Received: 9 June 2021 / Accepted: 12 August 2021 / Published online: 16 August 2021
© Akadémiai Kiadó, Budapest, Hungary 2021

Abstract

In this work, a series of cerium phosphate catalysts with different cerium phosphate molar ratios have been synthesized. The prepared catalysts were characterized by means of FTIR, DTA, TGA, XRD, N₂ adsorption–desorption and SEM. Also, the acidic centers of the prepared catalysts were abundantly studied and characterized in terms of type and strength using different techniques. The characterization tools used explained the variety of acidic centers in terms of type and strength due to the variation of cerium to phosphate molar ratio. Its worthy to mentioned that the highly acidic performance of the prepared catalysts was successfully applied in the synthesis of tetrahydrocarbazoles derivatives via Borsche–Drechsel cyclization reaction. The catalysts showed great catalytic activity in the selected reaction as high product yields were obtained using a very small amount of the catalysts under mild reaction conditions. The % yield and the reaction mechanism proves the role played by Brønsted acid sites of the catalyst in indorsing the reaction. The results also demonstrated a high ability of the catalysts to be reused ten times without a significant decrease in the catalytic activity. The synthesized tetrahydrocarbazole derivatives via heterogenous acid-catalyzed Borsche–Drechsel cyclization reaction can be considered as highly efficient and eco-friendly strategy towards many other carbazoles and open a new era in green chemistry as well.

Keywords Cerium phosphate · Acidic catalyst · Borsche–Drechsel reaction · Tetrahydrocarbazoles · Brønsted acidity

✉ Abdelrahman S. Khder
askhder@uqu.edu.sa

Extended author information available on the last page of the article

Introduction

In the last decades, the words “heterogeneous catalysis” is of the most used words in many scientific fields. Often these words (heterogeneous catalysis) are associated with other words, which are the “solid acid catalysts”. Whereas, mentioning these few words together has a great impact on both the environmental and economic aspects [1–7]. The replacement of industrial processes that are based on homogeneous catalysis to the technique of heterogeneous catalysis, as well as the use of solid acid catalysts instead of mineral acids such as HF, HCl, H₂SO₄, HNO₃,...etc. has a great positive impact on the environmental and economic aspects [8–12]. As these mineral acids cannot be reused, their corrosiveness, difficulties during using and their disposal by pumping into the surrounding environment has a great negative impact from an environmental and economic point of view. On the contrary, the use of solid acid catalysts and the possibility of reuse many cycles, and high ability to catalyze the reactions with high product yields, make such solid acid catalysts have a great positive impact from an environmental and economic point of view [13–18]. In this regard, many researchers have prepared different types of acidic solid catalysts that have been used in different industrial fields [1–4, 19, 20]. We have also previously and so far, prepared acidic solid catalysts which have proven highly effective in many industrial processes in an environmentally friendly manner [16–18, 21–23]. Amongst these catalysts are those containing oxoanions, tungstates and phosphates, which have demonstrated high catalytic activity [24–27]. The family of rare earth metal phosphates with general formula APO₄ (where A = rare earth metal) has different crystalline structures depending on the type of rare earth metal, preparation method, metal to phosphate ratio and calcination temperatures [28, 29]. As the precise control of these factors was found to have a great influence on both the structural and catalytic properties of these catalysts. Cerium phosphate (CeP) is one of the most important phosphates of the rare earth metals and has attracted many researcher’s attention due to its distinctive properties such as thermal stability, high surface area and high mechanical and ion exchange properties [30–32]. In addition, it has been found that rare earth metal phosphate contains different types of acid centers (Lewis and Brønsted) with different strengths, which can be used as a solid acid catalyst with high efficacy in many applications [26, 33]. The Brønsted acidity of cerium phosphate (CeP) is attributed to presence of P–OH groups, where Lewis acid sites are originated from Mn⁺ species [34, 35]. The acidic properties of cerium phosphate (CeP) can be easily attuned by controlling the preparation conditions, as well as the molar ratio of cerium to phosphate.

Borsche–Drechsel reaction, is an acid-catalyzed cyclization reaction that was firstly studied by Edmund Drechsel and Walter Borsche [36, 37]. The reaction was generally used for the synthesis of tetrahydrocarbazoles through the acid-catalyzed cyclization of cyclohexanone arylhydrazones. The tetrahydrocarbazoles derivatives are considered as excellent precursors for the synthesis of the enormous numbers of carbazoles derivatives with sound applications not only in medicinal chemistry but also in material science as well [38–41].

Herein, we will report the preparation of cerium phosphate (CeP) catalysts with different cerium: phosphate molar ratios via a direct solvothermal approach. The properties of the prepared catalysts will be studied using various characterization techniques. The catalytic activity will be assessed towards Borsche–Drechsel cyclization reaction to synthesize different tetrahydrocarbazole derivatives via green chemistry strategy and excellent precursors for the synthesis different substituted heterocyclic carbazole derivatives. The implemented strategy focused on leading the reaction under moderate conditions through an environmentally friendly protocol. In this issue, the prepared CeP acidic catalyst will be efficaciously used aiming to synthesize a unique family of organic compounds based on tetrahydrocarbazoles derivatives in the highest possible yield during the shortest possible time. We also cautiously studied the relationship between the catalyst composition, its acidity, and its catalytic activity.

Experimental

Materials

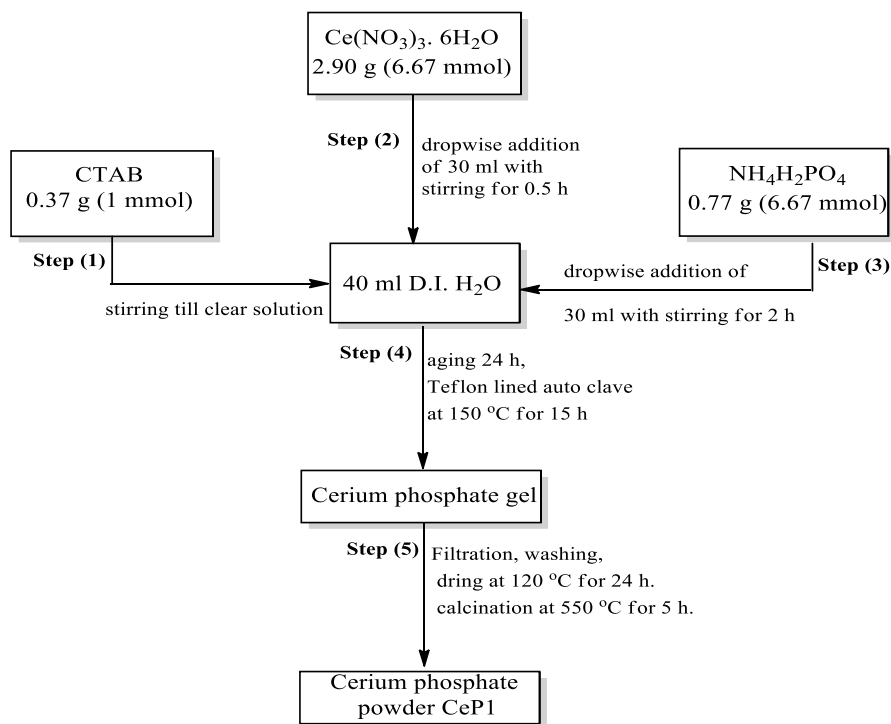
All the used chemicals were purchased from Sigma-Aldrich and used directly without further purification, including Cerium (III) nitrate hexahydrate ($\text{Ce}(\text{NO}_3)_3 \cdot 6\text{H}_2\text{O}$), ammonium dihydrogen phosphate ($\text{NH}_4\text{H}_2\text{PO}_4$), iodine and Cetyltrimethylammonium Bromide (CTAB). In addition, all organic precursors applied in the synthesis of tetrahydrocarbazole derivatives via acid catalyzed Borsche–Drechsel cyclization namely, absolute ethanol, cyclohexanone, 4-methylcyclohexanone, phenyl hydrazine, 4-methoxyphenyl hydrazine, 4-fluorophenyl hydrazine, 4-chlorophenyl hydrazine, 4-bromophenyl hydrazine, 4-iodophenyl hydrazine, 4-cyanophenyl hydrazine and 4-carboxyphenyl hydrazine were purchased from Merck and used as received without any further purifications.

Catalysts preparation and characterization

Cerium phosphate (CeP) was prepared by direct precipitation method in a total volume of 100 ml of D.I. H_2O in presence of cetyltrimethylammonium bromide (CTAB) as structure directing agent. Initially, calculated amount of CTAB was dissolved in 40 ml D.I. H_2O . Another two separate solutions each contains appropriate amount of Cerium (III) nitrate hexahydrate ($\text{Ce}(\text{NO}_3)_3 \cdot 6\text{H}_2\text{O}$), ammonium dihydrogen phosphate ($\text{NH}_4\text{H}_2\text{PO}_4$) in 30 ml D.I. H_2O were also prepared at room temperature. For the precipitation of CeP, first, 30 ml Cerium (III) nitrate hexahydrate solution was added to 40 ml CTAB solution and the mixture was stirred for 0.5 h. Then, 30 ml of ammonium dihydrogen phosphate solution was also added dropwise under vigorous stirring for 2 h. The pale-yellow gel obtained was aged overnight, then transferred to 200 ml Teflon lined autoclave and heated at 150 °C for 15 h. After cooling the autoclave to room temperature, the precipitate was filtered, washed several times with D.I. H_2O and dried at 120 °C for 24 h. The obtained powder was

grinded and calcined at 550 °C for 5 h using a heating rate of 1 °C min⁻¹. In the present study, 5 samples of CeP with different Ce: P molar ratios [1:0.5 (CeP0.5), 1: 1 (CeP1), 1:1.5 (CeP1.5), 1:2 (CeP2), 1: 2.5 (CeP2.5)] were prepared. The details preparation steps of cerium phosphate with Ce: P molar ratio 1: 1 (CeP1) are illustrated in Scheme 1.

The prepared CeP catalysts were characterized by using different techniques. FTIR spectra of the samples were recorded by using Shimadzu FTIR spectrophotometer in the range of 400 to 4000 cm⁻¹ with a resolution of 4 cm⁻¹. The thermal stability (thermogravimetric analysis (TGA) and differential thermal analysis (DTA) curves) of the dried catalysts were simultaneously recorded by using Shimadzu DTG-60 plus equipment using α -Al₂O₃ as standard. The dried catalyst was loaded in alumina pan and heated from room temperature to 800 °C with a heating rate of 10 °C min⁻¹ in N₂ atmosphere. The crystallinity and phase identification of the prepared catalysts was studied by using Philips X'Pert diffractometer equipped with copper radiation (Cu K α , λ =0.1541 nm) between 2 θ angles of 10° to 70°. Nitrogen adsorption-desorption measurements were carried out by using Quanta Chrome NOVA touch LX⁴. The morphology of the prepared catalysts was also studied by using scanning electron microscopy (SEM) (Quanta FEG 250, USA). Elemental analysis was performed to determine the real amounts of cerium, phosphorous existing in the prepared catalysts using inductive coupled plasma ICP-AES (Labtam,



Scheme 1 represented diagram for the preparation procedure of cerium phosphate (CeP1) catalyst

8440 Plasmalab). The surface acidities of the catalysts were entirely characterized by adopting two different techniques after the adsorption of pyridine (as prob base) over the catalysts surface. The type of acid sites (Lewis and/or Brønsted) were investigated by means of FTIR technique of pyridine bonded to the Lewis and Brønsted acid centers. The relative acid sites strength of the catalysts was also studied by adopting pyridine temperature-programmed desorption (Py-TPD) using Quantachrom Nova Chem BET Pulsar equipment. Prior to analysis, 0.1 g of the sample was charged in the equipment and heated up to 600 °C with a heating rate of 10 °C min⁻¹ in Ar atmosphere (50 ml min⁻¹).

Catalytic performance investigation

General procedures for the synthesis of tetrahydrocarbazoles by Borsche–Drechsel cyclization

In a typical synthetic methodology [42–45] in 50 ml round-bottom flask, a mixture of substituted phenyl hydrazine (10 mmol) in ethanol (10 ml) was added portion wise to the cyclohexanone derivatives (10 mmol) in ethanol (10 ml) for 10 min. The reaction mixture was refluxed to safeguard the complete reactants solubility (TLC-check at this point show no indication of product formation), then 0.02 g of the CeP catalysts were added under constant stirring and refluxing for the required reaction time and the reaction progress was monitored by thin layer chromatography. After reaction completed (TLC-controlled), the catalyst was removed by filtration and the solvent was removed under reduced pressure and the obtained product residue washed with cold ethanol to give the final pure product. The solid products obtained were chromatographically pure enough and no further purification required compared with authentic samples prepared via homogenous catalysis approach using acetic acid. The products were confirmed on the bases of both analytical and spectroscopic tools and find the data will fit with the previously established data. The obtained products were dried in vacuum drying oven and the product yield percentages (%) were calculate according to Eq. (1) [46]:

$$Yield (wt\%) = \frac{\text{actual weight of the product}}{\text{Theoretical weight of the product}} \times 100 \quad (1)$$

Results and discussion

Characterization of the prepared catalysts

The FTIR spectral technique is used to study the vibrational properties of the prepared samples. The FTIR spectra of CeP0.5, CeP1.5 and CeP2.5 samples calcined at 550 °C are show in Fig. S1. As seen in Fig. S1, the samples exhibit many vibrational bands between 400 and 4000 cm⁻¹. As is evident, all the catalysts exhibit a group of distinctive bands ascribed to phosphate groups. The FTIR bands observed

at 534, 565 and 615 cm^{-1} are ascribed to O–P–O, O–P and O=P–O bending vibrations of PO_4^{3-} group [47, 48]. Moreover, other bands are also observed at 950 and 1050 cm^{-1} are attributed to the asymmetric and symmetric stretching vibrations of P–O [31, 47]. The FTIR bands that observed at 1635 and 3450 cm^{-1} are ascribed to symmetric OH stretching and bending of water molecule, respectively [49]. The broad band at around 2375 cm^{-1} is attributed to P–O–H stretching vibration, which may be also responsible for Brønsted acidity [50]. The formation of polyphosphate structures in the CeP2.5 sample can be inferred from the band at 750 cm^{-1} , which is attributed to the P–O–P vibration [51]. In samples with lower phosphate content, such a band can hardly be observed. This may indicate that at higher phosphate content (CeP2.5), polyphosphate layers are formed on the catalyst surface. Moreover, Kijkawa et al. [29] noticed similar vibrational bands in FTIR spectra and attributed the reason for their emergence to a monazite structure formation of phosphates.

The effect of temperature on thermal decomposition and phase transitions of the as prepared samples have been studied by using simultaneous thermogravimetric and differential thermal analyses (DTA-TGA). Fig. S2 shows the collected thermograms of some cerium phosphate dried samples with different cerium: phosphate molar ratios. As it can be seen, the TGA curves (Fig. S2) of all samples exhibits different and successive stages of weight loss starting at room temperature to around 400 °C. Moreover, these stages of weight loss are also accompanied by some endothermic and exothermic changes, as shown in the DTA curves (Fig. S2). The first weight loss stage of around 5–6% started from room temperature up to 130 °C is accompanied with endothermic peaks which is ascribed to the loss of physically adsorbed water. The second weight loss step of around 2.5% occurs between 130 and 240 °C is also accompanied with another endothermic peak at the same temperature range is ascribed to the loss of chemically adsorbed water and formation of anhydrous cerium phosphate [52]. The third and final stage of weight loss from 4 to 5% extends to about 350 °C is accompanied by an exothermic effect, which is attributed to the removal of the residual nitrate, ammonia, and CETAB in the sample [31, 53]. After this stage, no thermal changes occur for all samples when heated to 800 °C, which means that all samples attain the thermal stability after 350 °C. Many authors indicated that there is an exothermic effect at elevated temperatures between 600 and 700 °C and is attributed to the cerium phosphate phase transition from hexagonal to monoclinic phase [48, 54–56]. In the present study, this exothermic peak at the higher temperatures is not observed, which may indicate the formation of the monoclinic structure at the as-prepared conditions.

The effect of the cerium to phosphate molar ratio on the crystal structure of the prepared samples that calcined at 550 °C is studied by the X-ray diffraction technique. Fig. 1 shows the X-ray diffractograms of all samples calcined at 550 °C. As shown in the figure, in the case of the lower molar ratio of phosphates compared to cerium (CeP0.5) the sample exhibits diffraction peaks corresponding to the cubic fluorite structure of the CeO_2 phase (JCPDS card no. 34-0394) [56]. In addition, when the molar ratio of cerium and phosphate are equal (CeP1), the sample exhibits a monazite type monoclinic phase of the cerium phosphate (JCPDS card no. 32-0199) [57]. Moreover, by further increasing in the phosphate to cerium molar ratio (CeP1.5, CeP2 and CeP2.5), no changes in the cerium

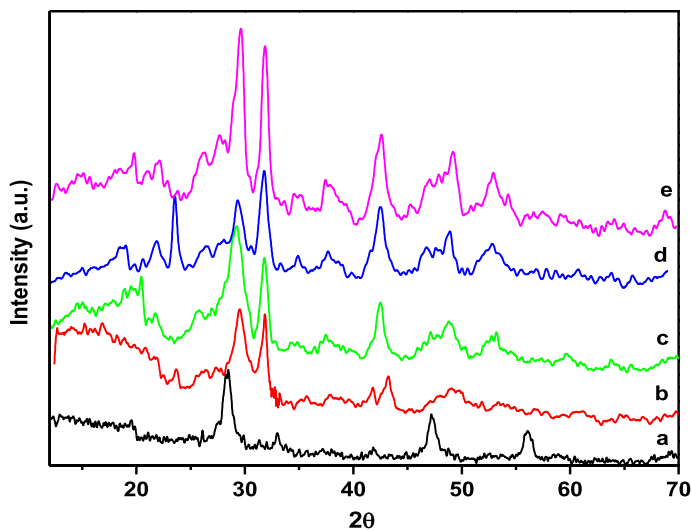


Fig. 1 XRD patterns of **a** CeP0.5, **b** CeP1, **c** CeP1.5, **d** CeP2 and **e** CeP2.5 samples calcined at 550 °C

phosphate monoclinic crystalline structure had observed. Where the samples exhibit similar diffraction peaks of cerium phosphate monoclinic crystalline structure with different peak intensities which indicate the preferential growth of cerium phosphate in specific directions. Moreover, the wide diffraction peaks may indicate the low degree of crystallinity of monoclinic cerium phosphate phase. It is also noted that both the X-ray diffraction, FTIR spectra and the thermal analysis results are consistent with the nature of the formation of a monoclinic phase with monazite-type of cerium phosphate.

The specific surface area (S_{BET}), total pore volume, average pore radius and average particle radius of the samples calcined at 550 °C are studied by nitrogen Adsorption–desorption at -196 °C. Fig. 2 displays the adsorption–desorption isotherms and the corresponding pore size distribution curves of all prepared catalysts. Moreover, the values of specific surface area (S_{BET}), total pore volume, average pore radius and average particle radius of the samples are listed in Table 1. As it can be seen, all the catalysts exhibit type IV adsorption–desorption isotherms rendering to IUPAC classification with H2 Type hysteresis loop which are characteristic for mesoporous material (Fig. 2). Moreover, the pore size distribution curves (Fig. 2 inset) of all catalysts show single peak with average pore radius between 3.6 and 5.0 nm which indicates that the pores are in the mesoporous range. The calculated values of specific surface area and total pore volume have maximum values of $101.6 \text{ m}^2 \text{ g}^{-1}$ and $0.254 \text{ cm}^3 \text{ g}^{-1}$ in case of equimolar cerium to phosphate ratio (CeP1). On the other hand, at higher phosphate to cerium molar ratio (CeP1.5) noteworthy decrease in both surface area and total pore volume values. Moreover, no distinguished changes in surface area and total pore volume values with further increase in the phosphate molar ratio. It is worth noting that the average particle radius (based on N_2 adsorption–desorption

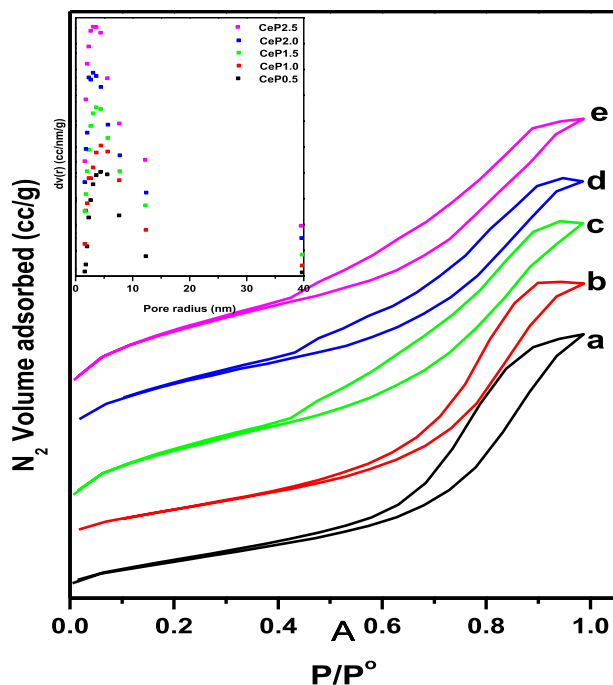


Fig. 2 N₂ adsorption–desorption isotherms and Pore volume distribution curves of **a** CeP0.5, **b** CeP1, **c** CeP1.5, **d** CeP2 and **e** CeP2.5 samples calcined at 550 °C

Table 1 Physicochemical properties of the prepared catalysts calcined at 550 °C

Sample	Elemental analysis		S _{BET} (m ² /g)	Total pore volume (cc/g)	Average pore radius (nm)	Average particle radius (nm)	Brønsted/Lewis ratio
	Ce (%)	P (%)					
CeP0.5	1.01	0.51	74.4	0.166	4.48	18.33	0.64
CeP1.0	0.99	1.02	101.6	0.254	5.00	13.42	0.90
CeP1.5	0.97	1.47	79.0	0.151	3.82	17.27	1.25
CeP2.0	1.03	1.99	71.1	0.132	3.63	18.78	1.20
CeP2.5	1.07	2.56	70.1	0.131	3.74	19.44	1.11

measurements) is less than 20 nm indicating that all catalysts have belonged to the nano category.

On the other hand, the morphology of the prepared catalysts was inspected by a scanning electron microscope (SEM). The images of some selected catalysts that calcined at 550 °C are presented in Figs. 3 and S3. It can be observed that CeP0.5 particles are mainly spherical in shape with an average size of around 0.75 μm (Fig. S3a). Moreover, the SEM images validate some changes in the morphology of the catalyst as a result of an increase in the phosphate molar ratio. In the CeP1 sample

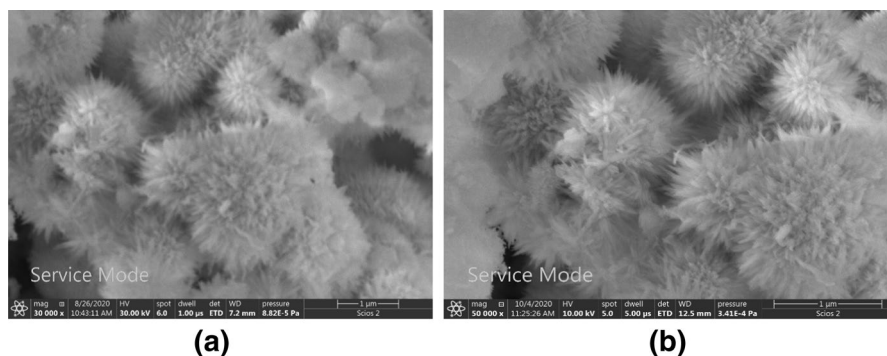


Fig. 3 SEM images of **a** CeP1.5, **b** CeP2.5 catalysts calcined at 550 °C

(Fig. S3b), the spherical morphology of the particles was also observed in addition to the appearance of some flower-like particles. Additionally, with further increase in the phosphate molar ratio, as is evident in CeP1.5 and CeP2.5 samples, the morphology of the flower-like particles becomes dominant (Figs. 3a, b). The scanning electron microscope (SEM) study confirms the effect of phosphate molar ratio on the morphology of the particles.

The FTIR spectra technique of chemisorbed pyridine has been used to study the surface acidities of all prepared catalysts that calcined at 550 °C. In this issue, we study the effect of phosphate content on the nature and distribution of acid sites of the prepared catalysts. According to the results represented in Fig. 4a, all the catalysts exhibit well defined FTIR spectral bands attributed to pyridine adsorbed on Lewis and Brønsted acid sites. Where all the catalysts show peak attributed to pyridine adsorbed at Lewis acid sites at 1450 cm^{-1} in addition to other peaks at 1540 and 1635 cm^{-1} which are attributed to pyridine adsorbed at Brønsted acid sites.

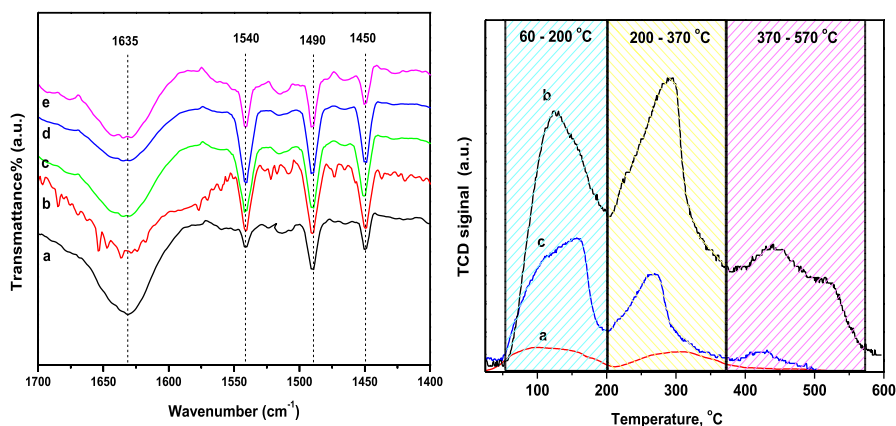


Fig. 4 **a** FTIR spectra of chemisorbed pyridine over **a** CeP0.5, **b** CeP1.0, **c** CeP1.5, **d** CeP2.0 and **e** CeP2.5, **b** Pyridine-TPD profiles over **a** CeP0.5, **b** CeP1.5 and **c** CeP2.5 samples calcined at 550 °C

Additionally, another peak at 1490 cm^{-1} , is observed which is ascribed to pyridine adsorbed on adjacent Lewis/Brønsted acid sites [22, 26]. Based on the peak area, the ratio of Brønsted/Lewis acid sites values (B/L) are calculated by using the peaks at 1540 and 1450 cm^{-1} , the results are listed in Table 1. As it can be seen in Fig. 4, both of Lewis and Brønsted acid sites are significantly enhanced as a result of phosphate addition. Moreover, the Brønsted/Lewis (B/L) ratio is augmented to the maximum value (1.25) when the cerium to phosphate molar ratio becomes 1.5 (CeP1.5) and thereafter decrease with further increase in the cerium to phosphate molar ratio (Table 1).

The results of the elemental analysis of the prepared samples by the ICP method were listed in Table 1. It is clear that the calculated molar ratio of cerium phosphate during the preparation was nearly the same as actual molar ratio in final product. This obviously revealed that all cerium and phosphate ions were almost completely precipitated.

The pyridine temperature programmed desorption (Py-TPD) technique is accomplished to the prepared catalysts owing to assess their relative acidity strength. According to the results displayed in Fig. 4b, three unique pyridine desorption regions can be observed that emphasize the presence of weak, moderate and strong acid sites. The first peak is observed between 50 and $200\text{ }^\circ\text{C}$, which is attributed to the desorption of pyridine adsorbed onto weak acidic sites that exist on the catalyst surface. Another desorption peak for the pyridine bonded to moderate acidic sites is observed within the temperature range 200 – $370\text{ }^\circ\text{C}$. Besides, another pyridine desorption peak is clearly observed at a higher temperature range (370 – $570\text{ }^\circ\text{C}$), which could be assigned to pyridine interacted with strong acidic sites. Careful inspection of Py-TPD profiles (Fig. 4b) reveals that: (i) all the selected catalysts exhibit the first two peaks that ascribed to desorption of pyridine bonded to weak and moderate acidic sites with different intensities, (ii) there is a severe deficiency of the strong acid centers on the surface of CeP0.5 catalyst, as evidenced by the absence of any pyridine desorption peak at higher temperatures, (iii) at the same time, this higher temperature desorption peak of pyridine in the other samples could be observed clearly with different intensities depending on the percentage of strong acidic centers in each sample, (iv) when the phosphate molar ratio increases, new strong acidic sites are created in addition to increasing the number of both weak and moderate acidic sites which reaches the maximum in CeP1.5 catalyst.

The study of the acidic properties of the catalysts elucidates the role played by phosphate species in the tuning of the acidic properties of the resultant catalysts. As the addition of phosphates is accompanied by the formation of some phosphate surface structures (as evident by FTIR study) such as PO_x and hydrated tetrahedral coordinated PO_4^{3-} (P–O–H) species which ultimately leads to the formation of more acid centers, especially of the Brønsted type [58, 59]. While, on the other hand, the formation of Lewis acid sites is mainly affected by the presence of unsaturated Mn^+ on the catalyst surface. The increase in the Brønsted/Lewis ratio as well as the strength of acid centers with the rise of phosphate content up to 1.5 (CeP1.5) is attributed to the gradual increase of P–O–H species on the surface. On the other hand, further increase in phosphate content leads to decrease in B/L ratio due to the formation of polytungstate species on the catalyst surface as a result of condensation

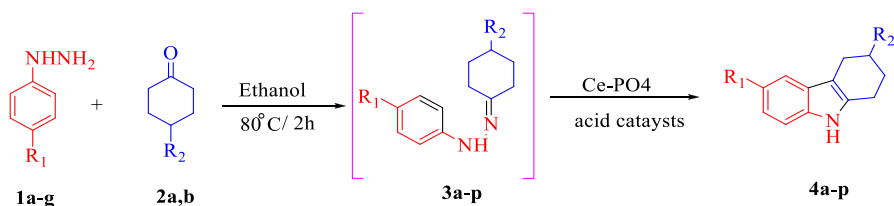
of two P–O–H groups into P–O–P group as evident from the appearance of FTIR band at 750 cm^{-1} .

Catalytic efficacy results (synthesis tetrahydrocarbazoles via Borsche–Drechsel cyclization)

The acidic heterogenous catalysis preparation of the tetrahydrocarbazole derivatives via Borsche–Drechsel cyclization reaction can be considered as unique, competent, expedient, and environmentally friendly protocol material chemistry. In this regard, the reaction was conducted in ethanol and under heterogenous mild reaction conditions (Scheme 2) and the obtained results are listed in Table 2.

It's worth mentioning that, the reaction was primarily carried out in absence of catalyst, using substituted phenylhydrazines and cyclohexanone in refluxing ethanol for 48 h (TLC controlled). Under catalyst free condition, no evidence for the formation of the tetrahydrocarbazole derivatives were monitored (Table 2, entry 1). This result confirms the role played by the acid catalyst in promoting the reaction. To enhance and prove the importance of the CeP acid catalysts in the Borsche–Drechsel cyclization, the reaction was carried to synthesis the parent 2,3,4,9-tetrahydro-1H-carbazole (**4a**) under the above-mentioned conditions at different reaction temperatures ($25\text{--}80\text{ }^{\circ}\text{C}$), in the presence of 0.02 g of the catalyst. Inspection of Table 2 (entry 2–21) Carefully reveals the following: (i) a highly pronounced yield of 2,3,4,9-tetrahydro-1H-carbazole is observed in presence of 0.02 g of all CeP catalysts, (ii) significant increase in the % yield of 2,3,4,9-tetrahydro-1H-carbazole when the phosphate molar ratio increases up to 1.5 in CeP1.5 where the % yield attains the maximum values at the selected reaction temperatures, (iii) further, an increase in phosphate molar ratio to 2 or 2.5 in CeP2 or CeP2.5 catalysts is accompanied by a notable decrease of 2,3,4,9-tetrahydro-1H-carbazole % yield.

The influence of dissimilar reaction parameters on the Borsche–Drechsel cyclization reaction was also premeditated to alter the reaction conditions. In this respect, to study the effect of reaction temperatures, the reaction was carried out in presence of 0.02 g of CeP catalysts for 2 h at 25, 40, 60 and $80\text{ }^{\circ}\text{C}$ (Table 2). The results show that at a lower temperature ($25\text{ }^{\circ}\text{C}$), low yield % of 2,3,4,9-tetrahydro-1H-carbazole (**4a**) is observed, which designate that the reaction needs more heat than this temperature and/or longer time to be completed. Additionally, when the reaction



Scheme 2 Schematic presentation of Borsche–Drechsel cyclization reaction for the synthesis of the tetrahydrocarbazole derivatives (**4a-p**) using CeP acid catalysis

Table 2 Optimization of the reaction condition for formation of 2,3,4,9-tetrahydro-1H-carbazole (**4a**) via Borsche–Drechsel cyclization reaction over CeP acid catalysts in ethanol for 2 h at different temperatures

Entry	Catalyst	Temp. (°C)	Time (h)	Yield (%)
1	No catalyst	80	48	0
2	CeP0.5	25	2	33.6
3	CeP0.5	40	2	66.3
4	CeP0.5	60	2	86.2
5	CeP0.5	80	2	94.3
6	CeP1	25	2	44.2
7	CeP1	40	2	67.6
8	CeP1	60	2	89.4
9	CeP1	80	2	95.9
10	CeP1.5	25	2	54.6
11	CeP1.5	40	2	73.5
12	CeP1.5	60	2	88.6
13	CeP1.5	80	2	99.6
14	CeP2	25	2	43.6
15	CeP2	40	2	67.3
16	CeP2	60	2	83.6
17	CeP2	80	2	96.5
18	CeP2.5	25	2	52.6
19	CeP2.5	40	2	66.3
20	CeP2.5	60	2	83.6
21	CeP2.5	80	2	95.9

temperature increases up to the refluxing temperature of ethanol (80 °C), the % yield is markedly increasing up to maximum values.

The effect of reaction time is one of the most important factors that affect the reaction, especially from an economic point of view. In this respect, we conducted the reaction for the synthesis of 2,3,4,9-tetrahydro-1H-carbazole over 0.02 g catalyst at 80 °C for 4 h, the results are presented in Fig. 5. As it can be seen, within the first two hours of the reaction time remarkable increase is the % yield of 2,3,4,9-tetrahydro-1H-carbazole was observed. Moreover, by additional increase in the reaction time, no further increase in the yield % of 2,3,4,9-tetrahydro-1H-carbazole were observed and predominantly decrease which may be due to some side reactions which are preferred at longer high temperature [60]. These results signify that, the reaction feasts to equilibrium state under the reaction conditions after nearly 2 h. On the other hand, Fig. 5 also displays that the conversion percentage was improved gradually with raising the amount of phosphate with cerium until reached a maximum conversion (99.6%) over CeP1.5 catalyst, which had a maximum surface acidity and highest Brønsted/Lewis Ratio (1.25), then decreases with further increase. From these results, the surface acidity or Brønsted/Lewis ratio has the great effect on the catalytic performance.

For economic and environment courtesies in heterogeneous catalysis, the permanence and reusability of the catalyst are very essential. In this issue, the reusability of the catalyst was explored over CeP1.5 sample under the same reaction conditions

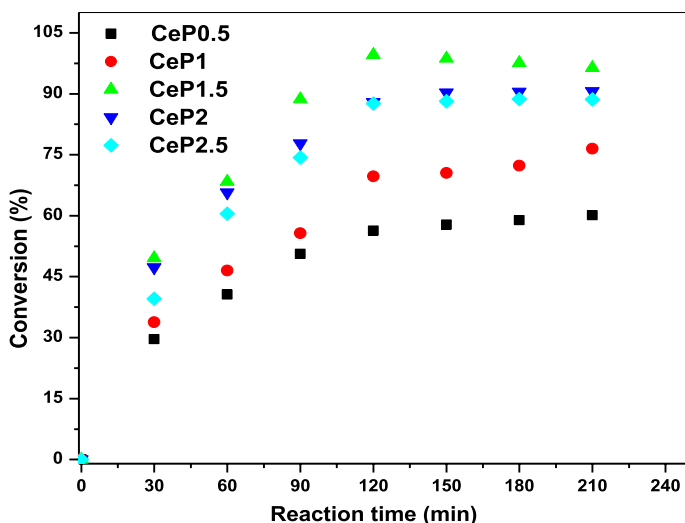


Fig. 5 Effect of reaction time on the % yield of 2,3,4,9-tetrahydro-1H-carbazole over 0.02 g catalyst at 80 °C

at 80 °C for 2 h, the results are shown in Fig. S4. Before recyclability study and after each run reaction, the catalyst is carefully removed from the reaction medium by filtration, washed with ethanol and dried under vacuum at 120 °C for 3 h and reused for the next run. The obtained results demonstrate that the catalyst could be recycled for at least 10 times without any pronounced loss of its acid catalytic activity, pre-tentious its high outstanding stability and reusability. Moreover, the leaching of the catalyst was studied after each reuse experiment of the CeP1.5 sample. In the issue, the amount of phosphorous (wt%) was measured using inductive coupled plasma ICP-AES technique, the results are cited in Table 1S. the results listed in Table 1S indicate that the catalyst is very stable against leaching even after 10 times of use.

We also studied the effect of substituents on the % yield of the synthesized tetrahydrocarbazole derivatives at the optimized reaction conditions (0.02 g catalyst, 2 h, at 80 °C) over CeP1.5 acid catalysis, the results are presented in Table 3 and Fig. S5. Its worthy to mention that, a pronounced increase in the yield % by approximately 5% of the tetrahydrocarbazole derivatives with the presence of electron donating groups substituted phenylhydrazines. More details for this observation will be given in details in the forthcoming paper.

It is very important to clarify that, the chemical structures of the synthesized tetrahydrocarbazoles via acid catalyzed Borsche–Drechsel cyclization reaction over CeP acid catalyst were conformed on the bases of both analytical and spectroscopic and tools and fond to well-fit with the previously reported data. For example, the IR-spectrum IR (ν cm^{-1}) of the 6-fluoro-3-methyl-2,3,4,9-tetrahydro-1H-carbazole (**4 k**) (Fig. S6) showed no evidence of the presence of NHNH_2 and $\text{C}=\text{O}$ of the starting materials and the following signals are shown up, a sharp signal at 3406 cm^{-1} corresponding to the NH group, at 3006 cm^{-1} for CH-aromatic, 2849 cm^{-1} for CH-aliphatic and at 1580 cm^{-1} for $\text{C}=\text{C}$. On the other hand, the ^1H NMR (600 MHz,

Table 3 Chemical structure and obtained yield at optimum conditions (80 °C for 2 h) of the synthesized tetrahydrocarbazoles **4a–p** over CeP1.5 acid catalysis

	Chemical structure	Yield %		Chemical structure	Yield %
4a		99.6	4i		94.3
4b		93.7	4j		91.7
4c		96.9	4k		94.2
4d		95.4	4l		93.5
4e		94.9	4m		90.9
4f		93.6	4n		86.4
4g		97.3	4o		94.7
4h		96.5	4p		93.6

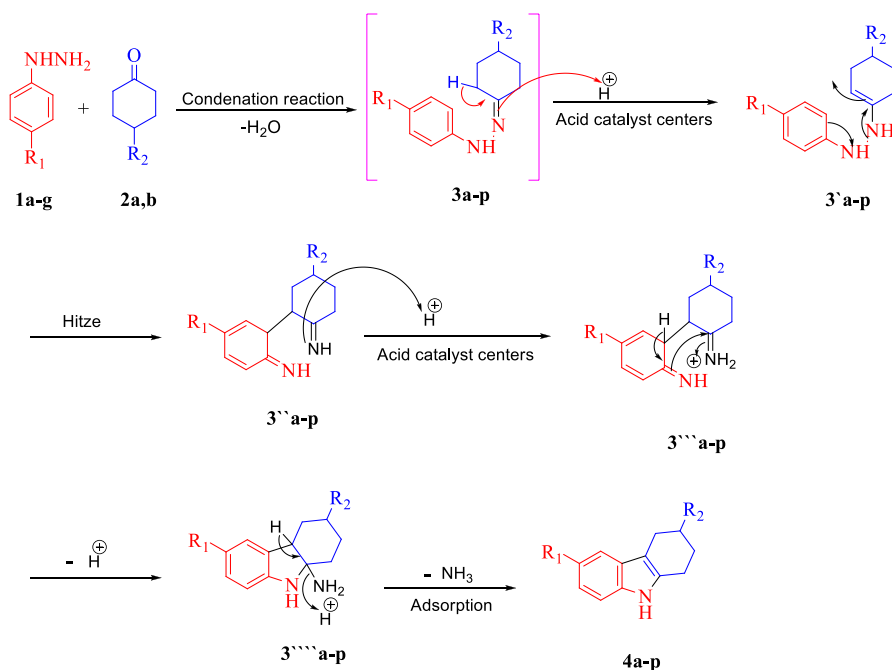
CHCl₃) of 6-fluoro-2,3,4,9-tetrahydro-1H-carbazole (**4c**) in CDCl₃ showed the following signals: δ 8.07 (s, D₂O, exchange, 1H), 7.82 (s, 1H), 7.28–7.32 (m, 2H), 2.79–2.82 (m, 4H), 1.50–1.81 (m, 4H). In addition, ¹³C NMR (125 MHz, CDCl₃): δ 134.4, 133.8, 128.7, 122.9, 120.9, 116.9, 113.8, 107.7, 27.3, 24.8, 23.3, 22.9 (Figs. S6, S7 and S8).

Commonly, Borsche–Drechsel cyclization reaction is a brilliant exemplary of acid catalyzed reaction which was studied by many authors [60–63]. The achieved results in the current study demonstrate the straightforward relationship between the acidic properties of the synthesized catalysts and their implementation in the clean synthesis of tetrahydrocarbazoles. Additionally, the obtained data show the unblemished effect of Brønsted-acidic centers on the catalytic efficiency of the reaction under investigation. These results are in good agreement with the earlier published results, which reveal the role of Brønsted acid centers in this reaction [64].

The reaction mechanism begins with elimination of water molecule because through condensation reaction of phenylhydrazines with cyclohexanone in the presence of Brønsted acid centers of the CeP catalysts to form to the condensation products, namely, cyclohexanone phenylhydrazones **3a-p**. Afterwards, a heat-induced sigmatropic reaction occurs to produce the intermediates **3'–3'''a-p**, which is protonated and cyclizes into **3''''a-p**, followed by elimination of ammonia to form the substituted tetrahydrocarbazole derivatives **4a-p** in high yield (Scheme 3).

Conclusions

In conclusion, cerium phosphate acid catalysts were prepared and characterized by many techniques. The study showed the effect of phosphate species on the textural and structural properties of cerium phosphate catalyst. Acidity measurement evidenced that the quantity, Brønsted and the strength of acid sites of the catalyst attained the maximum value at cerium: phosphate molar ratio of 1:1.5 and decreased thereafter. The catalysts also displayed unrepresented possibility for applications in some acid-catalyzed cyclization reactions. The catalysts were competently applied for Borsche–Drechsel cyclization reaction to synthesize tetrahydrocarbazole derivatives using a high efficiently acid-catalyzed reaction protocol, where more than 99% was obtained at 80 °C for 2 h over CeP1.5 catalyst. It's worth mentioning that the



Scheme 3 Proposed mechanistic pathway of Borsche–Drechsel cyclization reaction for the formation of the tetrahydrocarbazole derivatives (**4a-p**) under CeP acid catalysis

investigated catalysts could be reused many times without meaningful loss of their catalytic performance. These results stipulate that the synthesized catalysts can be measured as promising candidates and efficient catalysts for using in any related acid-catalyzed organic transformation reactions and can be proposed to open a new era in many industrial applications.

Supplementary Information The online version contains supplementary material available at <https://doi.org/10.1007/s11144-021-02050-4>.

Acknowledgements The authors are highly indebted to the Deanship of the Scientific Research (DSR), Umm Al-Qura University for the financial support through the Project Number 19-SCI-1-01-0010.


References

1. Liu Y, Guan Y, Li C et al (2006) Effect of ZnO additives and acid treatment on catalytic performance of Pt/WO₃/ZrO₂ for n-C7 hydroisomerization. *J Catal* 244:17–23
2. Lyon CJ, Sarsani VR, Subramaniam B (2004) 1-Butene+ isobutane reactions on solid acid catalysts in dense CO₂-based reaction media: experiments and modeling. *Ind Eng Chem Res* 43:4809–4814
3. Ahmed AI, El-Hakam SA, Samra SE et al (2008) Structural characterization of sulfated zirconia and their catalytic activity in dehydration of ethanol. *Colloids Surf A* 317:62–70
4. Arata K (1996) Preparation of superacids by metal oxides for reactions of butanes and pentanes. *Appl Catal A* 146:3–32
5. Salama RS, Mannaa MA, Altass HM et al (2021) Palladium supported on mixed-metal–organic framework (Co–Mn-MOF-74) for efficient catalytic oxidation of CO. *RSC Adv* 11:4318–4326
6. El-Hakam SA, Samra SE, El-Dafrawy SM et al (2018) Synthesis of sulfamic acid supported on Cr-MIL-101 as a heterogeneous acid catalyst and efficient adsorbent for methyl orange dye. *RSC Adv* 8:20517–20533. <https://doi.org/10.1039/c8ra02941e>
7. Salama RS, Hassan SM, Ahmed AI et al (2020) The role of PMA in enhancing the surface acidity and catalytic activity of a bimetallic Cr–Mg-MOF and its applications for synthesis of coumarin and dihydropyrimidinone derivatives. *RSC Adv* 10:21115–21128
8. Salama RS, El-Sayed E-SM, El-Bahy SM, Awad FS (2021) Silver nanoparticles supported on UiO-66 (Zr): as an efficient and recyclable heterogeneous catalyst and efficient adsorbent for removal of Indigo Carmine. *Colloids Surf A* 626:127089
9. El-Hakam SA, Samra SE, El-Dafrawy SM et al (2013) Surface acidity and catalytic activity of sulfated titania supported on mesoporous MCM-41. *Int J Mod Chem* 5:55–70
10. El-Hakam SA, Ibrahim AA, Elatwy LA et al (2021) Greener route for the removal of toxic heavy metals and synthesis of 14-aryl-14H dibenzo [a, j] xanthenes using a novel and efficient Ag-Mg bimetallic MOF as a recyclable heterogeneous nanocatalyst. *J Taiwan Inst Chem Eng*
11. Ibrahim AA, Salama RS, El-Hakam SA et al (2021) Synthesis of sulfated zirconium supported MCM-41 composite with high-rate adsorption of methylene blue and excellent heterogeneous catalyst. *Colloids Surf A* 616:126361
12. Salama RS, El-Hakama SA, Samra SE et al (2018) Cu-BDC as a novel and efficient catalyst for the synthesis of 3, 4-Dihydropyrimidin-2 (1H)-ones and Aryl-14H-dibenzo [a, j] Xanthenes under conventional heating. *Int J Nano Mater Sci* 7:31–42
13. Abd El Rahman SK, Hassan HMA, El-Shall MS (2012) Acid catalyzed organic transformations by heteropoly tungstophosphoric acid supported on MCM-41. *Appl Catal A* 411:77–86
14. Abd El Rahman SK, Hassan HMA, El-Shall MS (2014) Metal-organic frameworks with high tungstophosphoric acid loading as heterogeneous acid catalysts. *Appl Catal A* 487:110–118
15. El-Hakam SA, El-Khouly AA, Khder AS (1999) Effect of thermal treatment on various characteristics of nickel/aluminum phosphate catalysts. *Appl Catal A* 185:247–257
16. Ahmed AI, Samra SE, El-Hakam SA et al (2013) Characterization of 12-molybdophosphoric acid supported on mesoporous silica MCM-41 and its catalytic performance in the synthesis of hydroquinone diacetate. *Appl Surf Sci* 282:217–225

17. Abd El Rahman SK (2008) Preparation, characterization and catalytic activity of tin oxide-supported 12-tungstophosphoric acid as a solid catalyst. *Appl Catal A* 343:109–116
18. Khder AS, El-Sharkawy EA, El-Hakam SA, Ahmed AI (2008) Surface characterization and catalytic activity of sulfated tin oxide catalyst. *Catal Commun* 9:769–777
19. Wang S, Guin JA (2000) Silica-supported sulfated zirconia: a new effective acid solid for etherification. *Chem Commun* 2499–2500
20. Srivastava R, Iwasa N, Fujita S, Arai M (2008) Synthesis of nanocrystalline MFI-zeolites with intracrystal mesopores and their application in fine chemical synthesis involving large molecules. *Chem Eur J* 14:9507–9511
21. Ahmed AI, El-Hakam SA, Khder AS, El-Yazeed WSA (2013) Nanostructure sulfated tin oxide as an efficient catalyst for the preparation of 7-hydroxy-4-methyl coumarin by Pechmann condensation reaction. *J Mol Catal A* 366:99–108
22. Abd El Rahman SK, Ahmed SA, Khairou KS, Altass HM (2018) Competent, selective and high yield of 7-hydroxy-4-methyl coumarin over sulfonated mesoporous silica as solid acid catalysts. *J Porous Mater* 25:1–13
23. Hassan HMA, Betiha MA, Abd El Rahman SK et al (2016) Hafnium pentachloride ionic liquid for isomorphic and postsynthesis of HfKIT-6 mesoporous silica: catalytic performances of Pd/SO₄²⁻/HfKIT-6. *J Porous Mater* 23:1339–1351
24. Khder AS, Ahmed AI (2009) Selective nitration of phenol over nanosized tungsten oxide supported on sulfated SnO₂ as a solid acid catalyst. *Appl Catal A* 354:153–160
25. Altass HM, Abd El Rahman SK (2018) Preparation, characterization of highly active recyclable zirconium and tin tungstate catalysts and their application in Pechmann condensation reaction. *React Kinet Mech Cat* 125:227–243
26. Abd El Rahman SK, Ahmed SA, Altass HM (2016) Mesoporous metal (IV) phosphates as high performance acid catalysts for the synthesis of photochromic bis-naphthopyran via Claisen rearrangement. *React Kinet Mech Cat* 117:745–759
27. El-Hakam SA, El-Khouly AA, Khder AS (1999) Surface properties and catalytic activity of Ni/Al₂O₃–AlPO₄ catalysts. *Adsorp Sci Technol* 17:417–430
28. Li H, Zhang S, Zhou S, Cao X (2009) Bonding characteristics, thermal expansibility, and compressibility of RXO₄ (R= Rare Earths, X= P, As) within monazite and zircon structures. *Inorg Chem* 48:4542–4548
29. Kijkowska R, Cholewka E, Duszak B (2003) X-ray diffraction and Ir-absorption characteristics of lanthanide orthophosphates obtained by crystallisation from phosphoric acid solution. *J Mater Sci* 38:223–228
30. Qian L, Du W, Gong Q, Qian X (2009) Controlled synthesis of light rare earth phosphate nanowires via a simple solution route. *Mater Chem Phys* 114:479–484
31. Rajesh K, Mukundan P, Pillai PK et al (2004) High-surface-area nanocrystalline cerium phosphate through aqueous Sol–Gel route. *Chem Mater* 16:2700–2705
32. Kang J, Byun S, Nam S et al (2014) Synergistic improvement of oxygen reduction reaction on gold/cerium-phosphate catalysts. *Int J Hydrogen Energy* 39:10921–10926
33. Srilakshmi C, Ramesh K, Nagaraju P et al (2006) Studies on preparation, characterization and ammoxidation functionality of zirconium phosphate-supported V₂O₅ catalysts. *Catal Lett* 106:115–122
34. Hattori T, Ishiguro A, Murakami Y (1978) Acidity of crystalline zirconium phosphate. *J Inorg Nucl Chem* 40:1107–1111
35. Spielbauer D, Mekhemer GAH, Riemer T et al (1997) Structure and acidic properties of phosphate-modified zirconia. *J Phys Chem B* 101:4681–4688
36. Drechsel E (1888) Ueber Elektrolyse des Phenols mit Wechselströmen. *J für Prakt Chemie* 38:65–74
37. Borsche W (1908) Ueber Tetra- und Hexahydrocarbazolverbindungen und eine neue Carbazolsynthese. (Mitbearbeitet von. A. Witte und W. Bothe.). *Justus Liebigs Ann Chem* 359:49–80
38. Ackermann L, Born R, Álvarez-Bercedo P (2007) Ruthenium (IV) alkylidenes as precatalysts for direct arylations of alkenes with aryl chlorides and an application to sequential catalysis. *Angew Chem Int Ed* 46:6364–6367
39. Shou WG, Li J, Guo T et al (2009) Ruthenium-catalyzed intramolecular amination reactions of aryl- and vinylazides. *Organometallics* 28:6847–6854
40. Kajiyama D, Inoue K, Ishikawa Y, Nishiyama S (2010) A synthetic approach to carbazoles using electrochemically generated hypervalent iodine oxidant. *Tetrahedron* 66:9779–9784
41. Jordan-Hore JA, Johansson CCC, Gulias M et al (2008) Oxidative Pd (II)-catalyzed C–H bond amination to carbazole at ambient temperature. *J Am Chem Soc* 130:16184–16186

42. Humne V, Dangat Y, Vanka K, Lokhande P (2014) Iodine-catalyzed aromatization of tetrahydrocarbazoles and its utility in the synthesis of glycozoline and murrayafoline A: a combined experimental and computational investigation. *Org Biomol Chem* 12:4832–4836
43. Talukdar R (2019) BF₃·OEt₂ catalyzed base-free regioselective ring opening of N-activated azetidines with (E)-1-arylidene-2-arylhrazines. *J Iran Chem Soc* 16:127–136
44. Haag BA, Zhang Z, Li J, Knochel P (2010) Fischer indole synthesis with organozinc reagents. *Angew Chem Int Ed* 49:9513–9516
45. Park I-K, Suh S-E, Lim B-Y, Cho C-G (2009) Aryl hydrazide beyond as surrogate of aryl hydrazine in the Fischer indolization: the synthesis of N-Cbz-indoles, N-Cbz-carbazoles, and N, N'-Bis-Cbz-pyrrolo [2, 3-f] indoles. *Org Lett* 11:5454–5456
46. El-Dafrawy SM, Salama RS, El-Hakam SA, Samra SE (2019) Bimetal-organic frameworks (Cu-Cr100-x-MOF) as a stable and efficient catalyst for synthesis of 3, 4-dihydropyrimidin-2-one and 14-phenyl-14H-dibenzo [a, j] xanthenes. *J Mater Res Technol*
47. de Lima JF, Serra OA (2013) Cerium phosphate nanoparticles with low photocatalytic activity for UV light absorption application in photoprotection. *Dye Pigment* 97:291–296
48. Vinothkumar G, Lalitha AI, Suresh Babu K (2018) Cerium phosphate-cerium oxide heterogeneous composite nanozymes with enhanced peroxidase-like biomimetic activity for glucose and hydrogen peroxide sensing. *Inorg Chem* 58:349–358
49. Manna A, Altass HM, Salama RS (2021) MCM-41 grafted with citric acid: The role of carboxylic groups in enhancing the synthesis of xanthenes and removal of heavy metal ions. *Environ Nanotechnol Monit Manag* 15:100410. <https://doi.org/10.1016/j.enmm.2020.100410>
50. Sinhamahapatra A, Sutradhar N, Roy B et al (2010) Mesoporous zirconium phosphate catalyzed reactions: synthesis of industrially important chemicals in solvent-free conditions. *Appl Catal A* 385:22–30
51. Sinhamahapatra A, Sutradhar N, Roy B et al (2011) Microwave assisted synthesis of fine chemicals in solvent-free conditions over mesoporous zirconium phosphate. *Appl Catal B* 103:378–387
52. Lucas S, Champion E, Bregiroux D et al (2004) Rare earth phosphate powders REPO₄·NH₂O (Re= La, Ce or Y)—Part i. Synthesis and characterization. *J Solid State Chem* 177:1302–1311
53. Boakye EE, Hay RS, Mogilevsky P, Douglas LM (2001) Monazite coatings on fibers: II, coating without strength degradation. *J Am Ceram Soc* 84:2793–2801
54. Verma S, Bamzai KK (2014) Preparation of cerium orthophosphate nanosphere by coprecipitation route and its structural, thermal, optical, and electrical characterization. *J Nanoparticles*
55. Hanna AA, Mousa SM, Elkomy GM, Sherief MA (2010) Synthesis and microstructure studies of nano-sized cerium phosphates. *Eur J Chem* 1:211–215
56. Liu W, Feng L, Zhang C et al (2013) A facile hydrothermal synthesis of 3D flowerlike CeO₂ via a cerium oxalate precursor. *J Mater Chem A* 1:6942–6948
57. Asuvathraman R, Gnanasekar KI, Clinsha PC et al (2015) Investigations on the charge compensation on Ca and U substitution in CePO₄ by using XPS, XRD and Raman spectroscopy. *Ceram Int* 41:3731–3739
58. Yang F, Liu Q, Bai X, Du Y (2011) Conversion of biomass into 5-hydroxymethylfurfural using solid acid catalyst. *Bioresour Technol* 102:3424–3429
59. Kapoor MP, Inagaki S, Yoshida H (2005) Novel zirconium–titanium phosphates mesoporous materials for hydrogen production by photoinduced water splitting. *J Phys Chem B* 109:9231–9238
60. Zhang H, Zhou Z, Yao Z et al (2009) Efficient synthesis of pyrimidinone derivatives by ytterbium chloride catalyzed Biginelli-type reaction under solvent-free conditions. *Tetrahedron Lett* 50:1622–1624
61. Murata H, Ishitani H, Iwamoto M (2010) Synthesis of Biginelli dihydropyrimidinone derivatives with various substituents on aluminium-planted mesoporous silica catalyst. *Org Biomol Chem* 8:1202–1211
62. Oskooie HA, Heravi MM, Karimi N, Monjezy MH (2011) FeCl₃ immobilized in Al-MCM 41: an efficient catalyst system for the Biginelli reaction. *Synth Commun* 41:826–831
63. Kappe CO (2000) Recent advances in the Biginelli dihydropyrimidine synthesis. New tricks from an old dog. *Acc Chem Res* 33:879–888
64. Akhaja TN, Raval JP (2011) 1, 3-Dihydro-2H-indol-2-ones derivatives: Design, synthesis, in vitro anti-bacterial, antifungal and antitubercular study. *Eur J Med Chem* 46:5573–5579

Authors and Affiliations

Hatem M. Altass^{1,2} · **Abdelrahman S. Khder**^{1,2,3}  · **Saleh A. Ahmed**^{1,2,4} · **Moataz Morad**^{1,2} · **Abdullah A. Alsabei**^{1,2} · **Rabab S. Jassas**⁵ · **Khalid Althagafy**^{2,6} · **Awad I. Ahmed**³ · **Reda S. Salama**⁷

- ¹ Chemistry Department, Faculty of Applied Science, Umm Al-Qura University, Makkah 21955, Saudi Arabia
- ² Research Laboratories Unit, Faculty of Applied Science, Umm Al-Qura University, Makkah 21955, Saudi Arabia
- ³ Faculty of Science, Chemistry Department, Mansoura University, Mansoura 35516, Egypt
- ⁴ Chemistry Department, Faculty of Science, Assiut University, Assiut 71516, Egypt
- ⁵ Department of Chemistry, Jamoum University College, Umm Al-Qura University, Makkah 21955, Saudi Arabia
- ⁶ Physics Department, Faculty of Applied Science, Umm Al-Qura University, Makkah 21955, Saudi Arabia
- ⁷ Basic Science Department, Faculty of Engineering, Delta University for Science and Technology, Gamasa, Egypt